Acta Crystallographica Section D
Biological Crystallography
ISSN 0907-4449

Crystallization of the cytotoxic domain of a ribosome-inactivating colicin in complex with its immunity protein

Stephen Carr,[a]† Daniel Walker,[b]† Richard James,[b] Colin Kleanthous[b] and Andrew M. Hemmings[a,b]*

[a]School of Chemical Sciences, University of East Anglia, Norwich NR4 7TJ, England, and [b]School of Biological Sciences, University of East Anglia, Norwich NR4 7TJ, England

† These authors contributed equally to this work.

Correspondence e-mail: a.hemmings@uea.ac.uk

Received 25 April 2000
Accepted 31 July 2000

The complex between the ribonuclease domain of the ribosome-inactivating colicin E3 and its protein inhibitor, the cognate immunity Im3, has been crystallized and preliminary X-ray characterization has been performed. Single crystals of the 1:1 complex were grown from hanging-drop vapour-diffusion experiments using 2-propanol as a precipitant. The space group is $P3_121$ or $P3_221$, with unit-cell parameters $a = b = 93.7$, $c = 76.2$ Å. When cryocooled, these crystals diffract to a resolution of 2.4 Å. A search for suitable conventional heavy-atom derivatives was unsuccessful and so Im3 mutants containing engineered cysteine or methionine residues have been produced for mercury soaks and selenomethionine-labelling experiments, respectively.

1. Introduction

The colicins are plasmid-encoded antibacterial proteins produced by the Enterobacteriacae which are classified on the basis of the cell-surface receptor to which they bind. The E-class colicins bind to the *btuB* gene product, a receptor involved in the high-affinity transport of vitamin B_{12} in *Escherichia coli* (DiMasi *et al.*, 1973). This class has been further subdivided into nine immunity groups (Col E1–E9; Males & Stocker, 1982; Cooper & James, 1984) which exhibit four modes of cytotoxicity; cytoplasmic membrane depolarization (Col E1; Cramer *et al.*, 1990), specific cleavage of ribosomal RNA (Col E3, Col E4 and Col E6; Bowman *et al.*, 1971; Senior & Holland, 1971), cleavage of specific tRNAs (Col E5; Ogawa *et al.*, 1999) or non-specific cleavage of chromosomal DNA (Col E2, Col E7, Col E8 and Col E9; Schaller & Nomura, 1976; Toba *et al.*, 1988; Eaton & James, 1989; Chak *et al.*, 1991).

The ribonuclease (RNase) E3 colicin plasmids encode the 58 kDa toxin, a 9.5 kDa inhibitor protein (termed the immunity protein) which affords protection to the producing cell against the cytotoxic activity of the colicin and a 5.6 kDa lysis protein. Synthesis of these proteins in K12 strains of *E. coli* is under the control of the SOS promoter and as such is initiated by DNA damage (Pugsley & Schwartz, 1983). The expressed lysis protein causes partial cell lysis upon strong induction and is thought to be responsible for the release of the heterodimeric colicin complex into the extracellular medium.

The bacteriocidal activity of these colicins progresses through three distinct steps (receptor binding, translocation and cytotoxicity), each of which is associated with a specific domain in the toxin. Receptor binding involves the central domain of colicin E3 interacting with the BtuB receptor, while the subsequent translocation across the outer membrane involves the N-terminal domain of the toxin interacting with components of the *E. coli* tol translocation system (Lazdunski *et al.*, 1998). Once inside the cell, colicin E3 kills the target bacterium by ribosomal inactivation. *In vivo*, this involves a single nucleolytic break of 16S ribosomal RNA between bases 1493 and 1494 (Bowman *et al.*, 1971). The cytotoxic activity is associated with the 11.8 kDa C-terminal domain of the colicin (96 amino acids). This domain can be isolated as a stable folded protein and it is to this domain that the 84-residue immunity protein binds to form a stoichiometric complex that abolishes colicin activity (Ohno *et al.*, 1977).

The structures of a number of pore-forming colicins, colicin A (Parker *et al.*, 1989), colicin Ia (Wiener *et al.*, 1997) and colicin N (Vetter *et al.*, 1998), have been reported. Also, the DNase domains of colicins E9 and E7 in complex with their respective cognate immunities have been structurally characterized (Kleanthous *et al.*, 1999; Ko *et al.*, 1999). However, the structures of the RNase colicins remain unsolved. Structural data is however available for the colicin E3 immunity protein (Li *et al.*, 1999; Yajima *et al.*, 1993) and the crystallization of colicin E3 in complex with its immunity protein has been reported (Frolow & Shoham, 1990; Shoham & Djebli, 1992).

The aim of this study is to define the structure of the RNase domain of colicin E3 and to characterize the interaction with its cognate immunity protein (Im3). The 21.3 kDa complex has been crystallized and preliminary

X-ray analysis has been performed. Site-directed mutants of Im3 containing surface serine to cysteine or non-surface residue to methionine substitutions have been prepared for derivatization and crystallized using mercurous salts or for incorporation of selenomethionine, respectively.

2. Materials and methods

2.1. Protein expression and purification

The expression and purification of the colicin E3 RNase domain and immunity protein Im3 will be described elsewhere (Walker *et al.*, manuscript in preparation).

2.2. Crystallization and crystal characterization

Protein solution in 10 m*M* Tris–HCl pH 7.5 was concentrated to 45–50 mg ml^{-1} using an Amicon diafiltration device at 277 K. Initial crystallization screening experiments were carried out at both 277 and 281 K using the screens of Jancarik & Kim (1991) and Cudney *et al.* (1994) and the hanging-drop vapour-diffusion technique. Each experiment utilized a 4 µl drop containing equal volumes of concentrated protein solution and screen solution. Each hanging drop was equilibrated against a 700 µl reservoir of screen solution. Crystals were observed after several days from a screen solution containing 0.1 *M* sodium citrate pH 5.6, 20%(*v*/*v*) PEG 4K and 20%(*v*/*v*) 2-propanol at 277 K. Optimization around this condition involved the variation of pH in the range 5.0–6.0, PEG concentration between 0 and 30%(*v*/*v*), and 2-propanol concentration between 0 and 30%(*v*/*v*). All manipulations were carried out at 277 K.

For cryoprotection experiments, single crystals were soaked sequentially in crystallization solutions containing firstly 7.5%(*v*/*v*) ethylene glycol and then 15%(*v*/*v*) ethylene glycol. Both cryoprotection solutions also contained a concentration of PEG 4K that was 5%(*w*/*v*) greater than that found in the crystallization solution. Cryocooling was achieved by mounting single crystals in cryo-loops (Hampton Research, CA, USA) followed by either immediate immersion in a nitrogen-gas stream at 100 K, or by prior immersion into liquid nitrogen. Preliminary diffraction trials were carried out using a Rigaku R-AXIS IV area detector on an RU-200HB rotating copper-anode generator with focusing mirror optics operated at 50 kV, 100 mA. A native diffraction data set was also collected to 2.4 Å resolution at a wavelength of 0.95 Å on station 9.5 at the SRS (Daresbury, England). The data was processed and scaled using *DENZO* and *SCALEPACK* (Otwinoski & Minor, 1997).

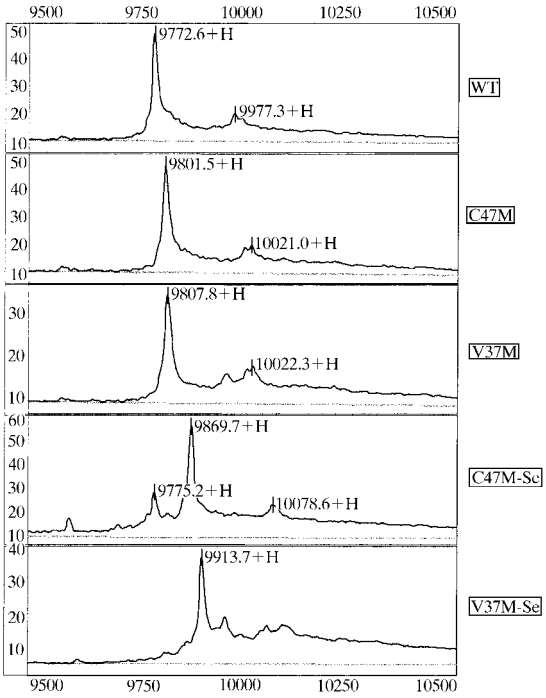

Figure 1
SELDI mass analysis of native Im3, C47M Im3, V37M Im3, Se-Met C47M Im3 and Se-Met V37M Im3.

2.3. Generation of derivatives for phasing experiments

In a search for heavy-atom derivatives, native crystals were soaked in 30 µl solutions of heavy-atom salts at various concentrations using sitting-drop vapour-diffusion conditions at 277 K. Other potential derivatives were produced by introducing mutations into the Im3 protein by mega-primer PCR mutagenesis (Sarker & Sommer, 1990). Firstly, cysteine mutants of Im3 were produced for derivatization with mercury and this involved the mutation of the native serine residues at positions 12, 30 or 69 to cysteine. Secondly, mutants containing engineered methionine residues were produced (native Im3 has a single methionine at position 32) with a view to producing selenomethionyl-labelled protein suitable for phasing the structure by multiple-wavelength anomalous dispersion (MAD) (*i.e.* selenomethionine at position 32 and also at the site of the mutation). The extra methionine was introduced at residue 37 (V37M mutant) or 47 (C47M mutant).

2.4. Preparation and analysis of selenomethionine-labelled Im3

Methionine-containing mutants were expressed and purified in the same manner as for the native Im3. Selenomethionine-labelled protein was expressed and purified as described elsewhere (Kühlmann *et al.*, 1999). To test for the incorporation of the desired mutation, the masses of samples of purified mutant Im3 proteins were measured using a PBS-II SELDI ProteinChip system (Ciphergen, UK) and compared with that expected from sequence analysis. The incorporation of selenium into selenomethionyl-derivatized protein was assayed by a comparison of the masses of selenium-containing methionyl-mutant proteins to those of the non-selenium-containing methionyl-mutant proteins.

X-ray fluorescence spectra were measured on station BM14 at the ESRF (Grenoble, France) using a single crystal of doubly labelled C47M selenomethionine-containing complex. Calculation of anomalous scattering factors from the raw fluorescence spectrum was performed using the *CHOOCH* program (Evans, 1998). Preliminary diffraction data were collected using an ADSC Quantum IV CCD detector at an X-ray energy of 12.66 keV (0.979 Å) and a crystal-to-detector distance of 185 mm. Indexing and data processing was performed using the *HKL* program suite (Otwinowski & Minor, 1997).

3. Results and discussion

Initial crystallization experiments using purified native colicin E3 RNase–Im3 complex produced large single crystals after 5 d in hanging-drop vapour-diffusion experiments. Variation of the 2-propanol concentration had no effect on crystal growth, but crystals only grew in the pH range 5.4–5.8. A reduction of the concentration of PEG 4K from 20 to 10%(*w*/*v*) was also required to reproducibly grow large crystals. PEG 4K was not critical for crystal growth and encouraged non-crystalline precipitation at higher concentrations. However, its presence greatly increased the stability of the crystals and rendered them less susceptible to cracking, although they still remained temperature sensitive. The

Table 1
Colicin RNase–immunity complex (E3–Im3) X-ray diffraction data-collection statistics.

Figures in parentheses refer to data in the highest resolution bin (2.55–2.4 Å resolution).

	Native E3–Im3	Se-Met E3–Im3 C47M
Wavelength (Å)	0.95	0.9795
Temperature (K)	100	100
Collected at	Station 9.5, SRS	Station BM14, ESRF
Space group	$P3_121$ or $P3_221$	$P3_121$ or $P3_221$
Unit-cell parameters (Å)	$a = b = 93.7$, $c = 76.2$	$a = b = 92.8$, $c = 77.2$
Resolution (Å)	2.4	2.8
Completeness (%)	98.7 (97.5)	99.2 (94.4)
$R_{\rm merge}$ (%)	3.9 (23.7)	5.4 (24.6)
$\langle I\rangle/\langle\sigma(I)\rangle$	37.8 (2.8)	21.1 (4.1)
Independent reflections	14892	9779

optimal condition was found to be 0.1 *M* sodium citrate pH 5.6, 20%(*v*/*v*) 2-propanol, 10%(*w*/*v*) PEG 4K; this produced crystals of typical dimensions 500 × 250 × 250 µm. SDS–PAGE analysis of proteins from serially washed crystals displayed three bands when stained with Coomassie blue rather than the expected two (data not shown). These correspond to the full-length Im3 and a doublet corresponding to the E3 RNase domain (freshly purified protein runs as a single band). Thus, the immunity protein appears stable to proteolytic degradation over the time course of the crystallization experiment, whereas the RNase appears to break down. The RNase gene construct used corresponds to residues Asp447–Leu551 of colicin E3 and it has been shown that Lys454 is a very permissive site in terms of proteolytic cleavage (Ohno *et al.*, 1977). It is therefore likely (although this has not been verified) that this is the site of the cleavage occurring during crystallization.

Cryoprotectant conditions were required as the crystals deteriorated very rapidly at room temperature. Good-quality diffraction was only observed when ethylene glycol was used as cryoprotectant and the greatest success was seen with crystals transferred sequentially into solutions of increasing ethylene glycol concentration.

Diffraction trials from crystals cryoprotected with 15%(*v*/*v*) ethylene glycol and mounted in cryoloops showed strong diffraction to 2.8 Å resolution. Autoindexing and consideration of systematically absent reflections reveal that the crystals belong to space group $P3_121$ or $P3_221$, with typical unit-cell parameters $a = b = 93.7$, $c = 76.2$ Å, $\alpha = \beta = 90$, $\gamma = 120^\circ$. Diffraction data collection from single crystals using synchrotron radiation gave a native data set to a maximum resolution of 2.4 Å (Table 1). Assuming the usual crystal solvent content, there may be one or two molecules per asymmetric unit. These correspond to calculated solvent contents of approximately 72 and 45%(*v*/*v*), respectively. The native crystals also displayed an inherent lack of isomorphism, which suggests that MAD phasing will be required to solve the structure.

Soaking native crystals in crystallization solutions containing 10 m*M* K_2PtBr_4 or 20 m*M* mercurous acetate followed by back-soaking into heavy-atom-free cryoprotectant solution produced crystals with X-ray fluorescence spectra characteristic of either Pt or Hg, respectively. This suggested incorporation of the heavy atoms into the crystal lattice. However, Patterson maps generated using the *CCP*4 program suite (Collaborative Computational Project, Number 4, 1994) from complete data sets collected at the optimal wavelength for anomalous scattering failed to locate any ordered heavy-atom sites. All other soaks resulted in crystal dissolution. The failure of this approach led us to prepare two classes of site-directed mutant of the Im3 protein that when complexed might lead to the incorporation of anomalous scatterers. These were (i) mutation of native serine residues to cysteine in order to facilitate mercury derivatization and (ii) mutation of various residues to methionine with a view to producing selenomethionyl-labelled protein. The Im3 protein already contains a single methionine residue at position 32, but this is the only native methionine present in the complex (removal of the N-terminal methionine occurs for both the ribonuclease domain and the immunity) and we were concerned that this would not provide sufficient phasing power to solve the structure of the 20 kDa complex. Therefore, in order to ensure the success of a selenomethionyl MAD experiment, extra methionine residues were engineered at residues 37 (Im3 V37M) and 47 (Im3 C47M) to give two single-site mutants.

Experiments aimed at the introduction of additional cysteine or methionine residues into the immunity protein were performed in parallel. The mutation of residue serine 12 to cysteine was performed (Im3 S12C) and its success verified by DNA sequencing (data not shown). Gel-filtration analysis was performed to ensure that complexation still occurred between the RNase domain and Im3 S12C. A single band corresponding to a species of apparent molecular weight 20 kDa was seen, demonstrating that Im3 S12C still bound the E3 RNase domain. Extensive rescreening around the native protein crystallization condition did not produce any crystals large enough for diffraction data collection for this mutant. Methionine mutants at both positions 37 and 47 were verified as such by SELDI (Fig. 1) and the masses of the mutants were found to be within 2–3 Da of the mass expected from sequence analysis (data not shown). The location of engineered methionine residues was decided by sequence homology between Im3, Im6 and Im4 (the latter two being immunity proteins for RNase colicins E6 and E4, respectively). In both homologous immunity proteins, there is a methionine residue at position 37 and the Im3 V37M mutant was therefore produced. Secondly, cysteine 47 has been shown to be involved in the binding of Im3 to E3 (Masaki *et al.*, 1991) and analysis of homologous sequences reveals this to be a mutational hot spot (for

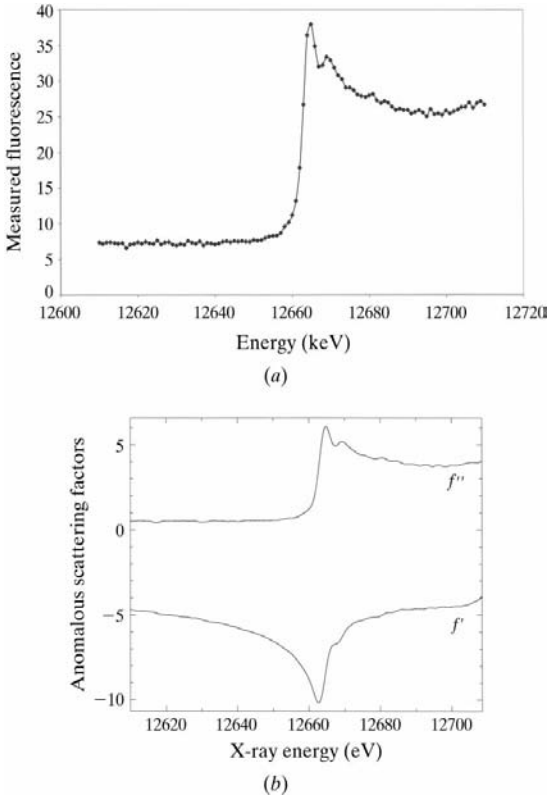

Figure 2
(*a*) X-ray fluorescence spectrum of a single crystal of Se-Met E3–Im3 C47M complex; (*b*) anomalous scattering factors determined from the spectrum in (*a*) as a function of X-ray energy.

example, this residue is a tryptophan in Im6) and so could potentially accommodate a methionine residue. Again, gel-filtration analysis verified complexation for both methionine mutants. Selenomethionine incorporation was successful for both mutants as verified by SELDI experiments and the results for Im3 C47M with and without selenium are presented in Fig. 1. Screening and optimization around the native crystallization condition failed to produce crystals when the complex contained Im3 V37M, but large single crystals were observed with the Se-Met E3–Im3 C47M complex.

The X-ray fluorescence spectrum was measured at the selenium *K* edge for an Se-Met E3–Im3 C47M complex crystal; calculated anomalous scattering factors as a function of X-ray energy are presented in Fig. 2. The anomalous scattering factors f' (inflection point) and f'' (peak) calculated from the measured fluorescence spectrum were −10.2 e at 12 662.6 eV and 6.1 e at 12 664.7 eV, respectively. The diffraction images collected from this crystal showed diffraction to 2.8 Å. The clearly resolved selenium *K* edge apparent from the fluorescence spectrum together with the quality of the diffraction from this crystal indicate that a selenium MAD phasing experiment is likely to be successful.

We acknowledge access to the BM14 beamline at the ESRF, Grenoble and to SRS station 9.5, Daresbury Laboratory. We would like to acknowledge the contribution of Dr Gordon Leonard (ESRF) for assistance with measurements of X-ray fluorescence spectra.

References

Bowman, C. M., Dahlaberg, J. E., Ikemura, T., Konisky, J. & Nomura, M. (1971). *Proc. Natl Acad. Sci. USA*, **68**, 964–968.
Chak, K.-F., Kuo, W.-S., Lu, F.-M. & James, R. (1991). *J. Gen. Microbiol.* **137**, 91–100.
Collaborative Computational Project, Number 4 (1994). *Acta Cryst.* D**50**, 760–763.
Cooper, P. C. & James, R. (1984). *J. Gen. Microbiol.* **130**, 209–215.
Cramer, W. A., Cohen, F. S., Merril, A. R. & Song, H. Y. (1990). *Mol. Microbiol.* **4**, 519–526.
Cudney, R., Patel, S., Weisgraber, K., Newhouse, Y. & MacPherson, A. (1994). *Acta Cryst.* D**50**, 414–423.
Di Masi, R. D., White, J. C., Schnaitman, C. A. & Bradbeer, C. (1973). *J. Bacteriol.* **115**, 506–513.
Eaton, T. & James, R. (1989). *Nucleic Acids Res.* **17**, 1761–1761.
Evans, G. (1998). *CHOOCH. A Program for Calculating Anomalous Scattering Factors from X-ray Fluorescence Data.* http://lagrange.mrc-lmb.cam.ac.uk/doc/gwyndaf/Chooch.html.
Frolow, R. & Shoham, M. (1990). *J. Biol. Chem.* **265**, 10196–10197.
Jancarik, J. & Kim, S.-H. (1991). *J. Appl. Cryst.* **24**, 409–411.
Kleanthous, C., Kühlmann, U. C., Pommer, A. J., Ferguson, N., Radford, S. E., Moore, G. R., James, R. & Hemmings, A. M. (1999). *Nature Struct. Biol.* **6**, 243–251.
Ko, T.-P., Liao, C.-C., Ku, W.-Y., Chak, K.-F. & Yuan, H. S. (1999). *Structure*, **7**, 91–102.
Kühlmann, U. C., Kleanthous, C., James, R., Moore, G. R. & Hemmings, A. M. (1999). *Acta Cryst.* D**55**, 256–259.
Lazdunski, C. J., Bouveret, E., Rigal, A., Journat, L., Lloubes, R. & Benedetti, H. (1998). *J. Bacteriol.* **180**, 4993–5002.
Li, C., Zhao, D., Djebli, A. & Shoham, M. (1999). *Structure*, **7**, 1365–1372.
Males, B. M. & Stocker, B. A. D. (1982). *J. Gen. Microbiol.* **128**, 95–106.
Masaki, H., Akutsu, A., Uozumi, T. & Ohta, T. (1991). *Gene*, **107**, 133–138.
Ogawa, T., Tomita, K., Ueda, T., Watanabe, K., Uozumi, T. & Masaki, H. (1999). *Science*, **283**, 2097–100.
Ohno, S., Ohno-Iwashita, Y., Suzuki, K. & Imahori, K. (1977). *J. Biochem.* **82**, 1045–1053.
Otwinowski, Z. & Minor, W. (1997). *Methods Enzymol.* **276**, 307–326.
Parker, M. W., Pattus, F., Tucker, A. D. & Tsernoglou, D. (1989). *Nature (London)*, **337**, 93–96.
Pugsley, A. P. & Schwartz, M. (1983). *Mol. Gen. Genet.* **190**, 366–372.
Sarker, G. & Sommer, S. S. (1990). *Biotechniques*, **8**, 404–407.
Schaller, K. & Nomura, M. (1976). *Proc. Natl Acad. Sci. USA*, **73**, 3989–3993.
Senior, B. W. & Holland, I. B. (1971). *Proc. Natl Acad. Sci. USA*, **68**, 959–963.
Shoham, M. & Djebli, A. (1992). *Bacteriocins, Microcins and Lantibiotics*, NATO ASI Series, Vol. H65, edited by R. James, C. Lazdunski & F. Pattus, pp. 203–214. Berlin: Springer–Verlag.
Toba, M., Masaki, H. & Ohta, T. (1988). *J. Bacteriol.* **170**, 3237–3242.
Vetter, I. R., Parker, M. W., Tucker, A. D., Lakey, J. H., Pattus, F. & Tsernoglou, D. (1998). *Structure*, **6**, 863–874.
Wiener, M., Freymann, D., Ghosh, P. & Stroud, R. M. (1997). *Nature (London)*, **385**, 461–464.
Yajima, S., Muto, Y., Morikawa, S., Nakamura, H., Yokoyama, S., Masaki, H. & Uozumi, T. (1993). *FEBS Lett.* **333**, 257–260.